

Chapter 1

Introduction to Dark Matter



Derek F. Jackson Kimball and Dmitry Budker

Abstract To set the stage for our study of ultralight bosonic dark matter (UBDM), we review the evidence for the existence of dark matter: galactic and stellar dynamics, gravitational lensing studies, measurements of the cosmic microwave background radiation (CMB), surveys of the large-scale structure of the universe, and the observed abundance of light elements. This diverse array of observational evidence informs what we know about dark matter: its universal abundance, its spatial and velocity distribution, and that its explanation involves physics beyond the Standard Model. But what we know about dark matter is far outweighed by what we do not know. We examine UBDM in the context of several of the most prominent alternative hypotheses for the nature of dark matter: weakly interacting massive particles (WIMPs), sterile neutrinos, massive astrophysical compact halo objects (MACHOs), and primordial black holes (PBHs). Finally we examine some of the key general characteristics of UBDM, including its wavelike nature, coherence properties, and couplings to Standard Model particles and fields.

1.1 Why Do We Think There Is Dark Matter?

Scientists have long speculated that there may be imperceptible forms of matter in the universe. Indeed, time and again forms of matter previously unknown have been discovered: Galileo used the telescope to discover the moons orbiting Jupiter, Chadwick irradiated a beryllium target to discover the neutron, Cowan and Reines used a water tank surrounded with scintillators to directly observe the neutrino flux

D. F. Jackson Kimball (✉)
Department of Physics, California State University, East Bay, Hayward, CA, USA
e-mail: derek.jacksonkimball@csueastbay.edu

D. Budker
Helmholtz Institut Mainz, Johannes Gutenberg-Universität, Mainz, Germany
Department of Physics, University of California, Berkeley, CA, USA
e-mail: budker@uni-mainz.de

from a nuclear reactor, and so on. But the story of “dark matter” as we understand it today begins with early efforts by Kelvin, Poincaré, Öpik, Kapteyn, and Oort to use the dynamics of the stars in the Milky Way to estimate the ratio of the mass of luminous matter (stars) to the total mass of matter in the galaxy (see the historical review [1] and the references therein).

While these early estimates [2, 3] found that stars dominated the mass in our local solar neighborhood, Zwicky [4, 5] used observations of galaxy clusters to discover that on much larger scales it appeared that *dunkle Materie* (German for *dark matter*) was considerably more abundant than luminous matter. Zwicky analyzed the Coma cluster, which had roughly a thousand galaxies distributed in a sphere of radius $R \approx 10^6$ ly. Each galaxy in the Coma cluster contained, on average, stars whose total mass was $M_{\text{tot}} \sim 10^9 M_{\odot}$ (where M_{\odot} is a solar mass), based on the mass/luminosity ratio determined from stars in our local solar neighborhood. From this information, the velocity dispersion of the galaxies can be predicted using the virial theorem

$$\langle K \rangle = -\frac{1}{2} \langle V \rangle, \quad (1.1)$$

where $\langle K \rangle$ is the time-averaged kinetic energy of the galaxies and $\langle V \rangle$ is the time-averaged gravitational potential energy. This estimate yields a velocity dispersion of

$$v \approx \sqrt{\frac{G_N M_{\text{tot}}}{R}} \approx 10^5 \text{ m/s}, \quad (1.2)$$

where G_N is the Newtonian constant of gravitation. However, the measured velocity dispersion of the galaxies in the Coma cluster was $\approx 10^6$ m/s, an order-of-magnitude discrepancy. It was later discovered that galaxy clusters contain a halo of hot gas with five times the mass of the stars [6, 7]: taking this into account reduced but did not eliminate the discrepancy between the predicted and observed velocity dispersion [8].

The next significant clues about the existence of dark matter came from observations of galactic rotation curves, the rotational velocity v of galaxies’ stars as a function of their distance r from the galactic center. The mass distribution within galaxies can be inferred from the rotation curves, as discussed in Problem 1.1. Pioneering observations of numerous galaxies by astrophysicists Vera Rubin, Kent Ford, and others [9–13] showed that past the radius within which most of the luminous matter is concentrated, the rotation curves are typically flat: v is relatively independent of r (as seen in Fig. 1.1). This is in marked contrast to the expected $1/\sqrt{r}$ dependence of v on r if luminous matter alone is the source of the gravitational pull holding outer stars in their orbits (see Problem 1.1). These rotation-curve observations can be explained by the galactic masses being dominated by a spherical halo of dark matter extending far beyond the luminous matter of galaxies.

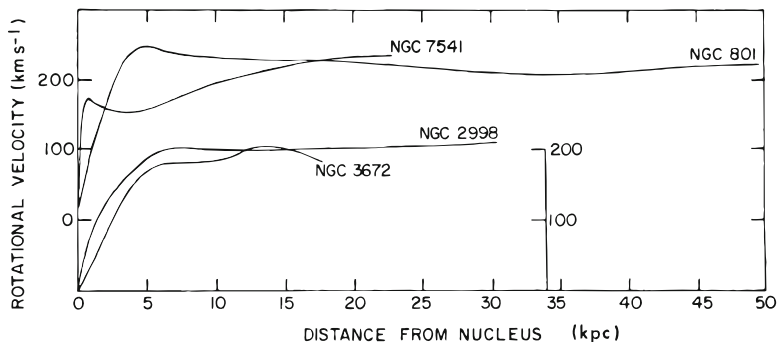


Fig. 1.1 Plot adapted from one of Rubin and Ford’s papers, Ref. [13], showing the rotational velocity as a function of distance from the galactic centers (nuclei) of four different galaxies (NGC 7541, NGC 801, NGC 2998, and NGC 3672), all of which exhibit flat rotation curves

? Problem 1.1 Galactic Rotation Curves

Consider a star in a circular orbit at the periphery of a galaxy of mass M , such that most of the galaxy’s mass is contained within the star’s orbital radius R . How does the star’s orbital velocity scale with R under these assumptions? Given that we observe flat galactic rotation curves, what can we assume is the radial dependence of the dark matter density?

Solution on page 305.

Gravitational lensing studies (see Refs. [14, 15] for reviews) considerably strengthened the case for the existence of dark matter. Because a gravitational field bends the otherwise straight-line trajectory of light, mass can distort the images of distant astrophysical objects as light travels along geodesics from those objects to the Earth. Since the images are distorted in predictable ways based on general relativity, gravitational lensing offers an independent method to investigate the distribution of mass in the universe. In 2006, Clowe et al. used gravitational lensing to study the Bullet Cluster (1E0657-558) [16], a pair of galaxy clusters that had merged ≈ 150 million years ago. Comparison of gravitational lensing to observations of stars and hot x-ray emitting gas established that the mass distribution of the Bullet Cluster does not coincide with the baryon distribution (Fig. 1.2). As seen in Fig. 1.2, the baryonic matter (dominated by hot gas, imaged by detection of x-ray emission) is clumped more closely together than the total mass of the cluster (measured by gravitational lensing), which is centered about two widely separated positions. Evidently when the two galaxy clusters merged, the baryonic matter collided and heated up while the dark matter barely interacted at all: the dark matter passed through the clusters without any observable effect, save that due to

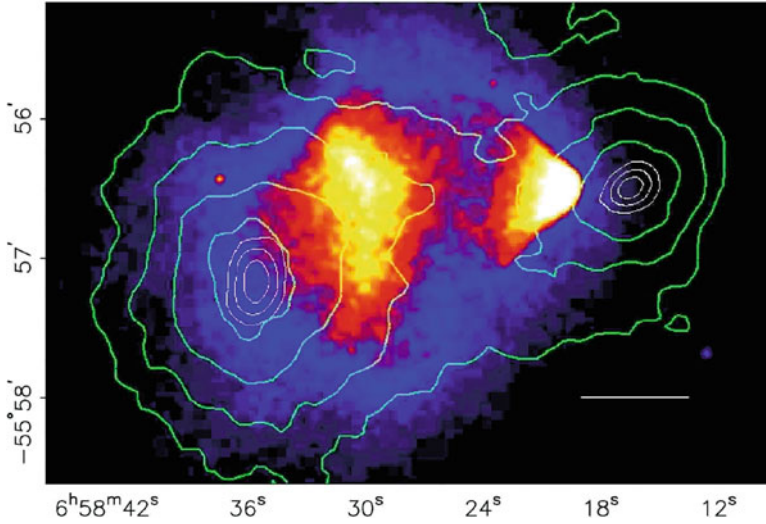


Fig. 1.2 Image of the Bullet Cluster (1E0657-558), adapted from Ref. [16], comparing x-ray emission from hot gas [the background color map with increasing x-ray intensity scaling from blue (low) to yellow/white (high)] to the mass distribution deduced from gravitational lensing (green contour plot, where the outermost contour represents low mass density and the innermost contours are highest density). The white horizontal line in the lower right represents a distance of 200 kpc at the position of the Bullet Cluster. The mass distribution is clearly different from the gas distribution

gravity. This is strong evidence that dark matter is not ordinary baryonic matter, and has been confirmed by further observations of other galaxy cluster mergers [17].

Measurements of the cosmic microwave background radiation (CMB) also point to the existence of dark matter. The CMB is a photon gas permeating the universe that essentially decoupled from baryonic matter $\approx 400,000$ years after the Big Bang. This time, known as *recombination*,¹ is when the universe had cooled to the point where the first atoms formed. From the appearance of baryons until recombination, the plasma of protons, electrons, and photons strongly interacted via Compton scattering and formed a coupled photon-baryon fluid. Thus the photons and baryons shared similar spatial patterns of density. After recombination the photons largely decoupled from baryonic matter. This is because the interaction of light with neutral atoms (integrated over all frequencies²) is strongly suppressed compared to the interaction of light with free charged particles. The observed CMB photons are relics

¹ The term *recombination* is somewhat misleading, since protons and electrons were not previously “combined”—recombination is a historical name established prior to the widespread acceptance of the Big Bang theory.

² Although light can strongly interact with neutral atoms at particular resonance frequencies, such resonant light-atom interactions produce spectral distortions of the CMB that are too small to detect at present [18, 19].

that provide a picture of the photon-baryon fluid at the *surface of last scattering* (the region of space a distance from which the photons from recombination have freely travelled to reach the Earth today). The CMB photons impinge on the Earth nearly uniformly from all directions and almost perfectly match a blackbody spectrum. However, there are relatively small fluctuations in the temperature and polarization of the CMB from different regions of the sky. The CMB fluctuations observed today are imprints of the photon-baryon density distribution at the time of recombination [20–22].

Based on the predictions of general relativity, cosmologists expect that the spatial fluctuations of matter density $\delta\rho_m$ should grow linearly with the expansion of the universe from the time of recombination up until the time at which $\delta\rho_m/\rho_m \gtrsim 1$. More precisely, as long as $\delta\rho_m/\rho_m \lesssim 1$, then $\delta\rho_m/\rho_m \propto a$, where a is the scale factor (see Refs. [23–25] for derivations of this relationship). The scale factor a relates the distance $d(t)$ between objects in the universe at a time t to the distance between the objects at the present time t_0 :

$$d(t) = ad(t_0) \quad (1.3)$$

and is related to the redshift z of light emitted from an object at time t by

$$a = \frac{1}{1+z} . \quad (1.4)$$

Thus as the universe expands, the density fluctuations grow: $\delta\rho_m/\rho_m \propto a$; or, conversely, the density fluctuations observed at high redshift ($z \gg 1$) should be proportionally smaller: $\delta\rho_m/\rho_m \propto 1/z$.

An overdense region of space where $\delta\rho_m/\rho_m \gtrsim 1$ will undergo gravitational collapse, forming regions of significant overdensity: the galaxies and galactic clusters that we observe in the present epoch [26]. Recombination occurred at a redshift of $z \approx 1100$, and thus $\delta\rho_m/\rho_m$ has grown by a factor of $\approx 10^3$ since then. In order for the observed galaxy distribution throughout the universe to have grown from the density fluctuations at the moment of recombination, $\delta\rho_m/\rho_m$ at recombination should be at the level of a part per hundred³ [28]. Measurements show, however, that the CMB is remarkably uniform throughout the sky (to more than a part in $\approx 10^5$), reflecting a similarly uniform baryon density at recombination. Thus galaxy formation could not possibly be seeded by the fluctuations in baryon density at recombination: $\delta\rho_m/\rho_m$ would be only $\lesssim 10^{-2}$ today and matter would still not have undergone gravitational collapse to form galaxies.

These apparently contradictory observations can be reconciled if the mass of baryonic matter in the universe is small compared to the mass of a gas of nonrelativistic (cold) dark matter particles that weakly interact with baryonic matter. This cold dark matter (CDM) could have begun clumping long before recombination.

³ The first stars and galaxies appear at a redshift of $z \gtrsim 10$ [27].

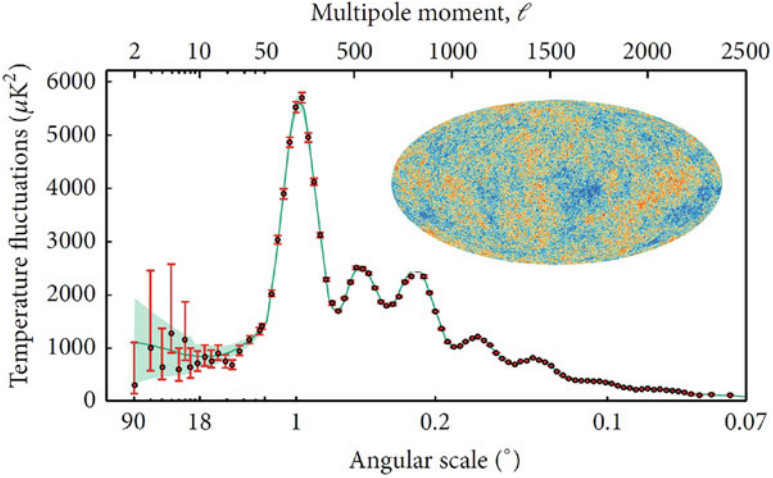


Fig. 1.3 Plot of the angular anisotropy of the square of the CMB temperature fluctuations in terms of multipole moments $\propto \langle |a_{\ell m}|^2 \rangle$ (averaged over m) and associated angular scale. Figure adapted from Ref. [35]. The black dots with red error bars are data from the Planck satellite observations and the green curve is the theoretical fit. The oval inset shows the Planck all-sky map of the CMB intensity fluctuations. The agreement between theory and data from the Planck and WMAP missions supports a flat universe whose matter density is dominated by CDM [32–34]

Thus by the time of recombination the CDM could have relatively large density fluctuations, whereas the baryons were still nearly uniformly distributed at that point in time [29]. The hot photon-baryon fluid would pass through the “clumpy” CDM with relatively little perturbation (resembling the case of the Bullet Cluster discussed above). Thus the photon-baryon fluid at recombination, and hence the CMB, exhibit small fluctuations while the large density fluctuations of the CDM could seed the formation of galaxies and give rise to the highly nonuniform distribution of matter observed today [30, 31].

This description can be made quantitative by calculating and measuring the variation of the CMB temperature $\delta T(\theta, \phi)$ across the sky, where θ and ϕ indicate the angular position. In terms of spherical harmonics $Y_{\ell m}(\theta, \phi)$:

$$\delta T(\theta, \phi) = \sum_{\ell, m} a_{\ell m} Y_{\ell m}(\theta, \phi), \quad (1.5)$$

where $a_{\ell m}$ is the expansion coefficient of the CMB temperature associated with the respective $Y_{\ell m}(\theta, \phi)$. Measurements of the angular anisotropy spectrum of the CMB by the WMAP (Wilkinson Microwave Anisotropy Probe) and Planck missions [32, 33] agree with theoretical predictions based on a cosmology with a CDM-dominated matter density [33, 34]. Data from the Planck mission are shown in Fig. 1.3.

The peaks in the plot of the angular anisotropy of the CMB temperature fluctuations appearing at different ℓ seen in Fig. 1.3 reveal both the underlying

spacetime geometry of the universe and the baryon density [36], as we explain below. The peaks in Fig. 1.3 are a result of the so-called *baryon acoustic oscillations* (BAO). Baryonic matter falls into the gravitational potential wells created by concentrations of CDM, but as the baryons fall into the potential wells and the plasma density increases, the plasma heats up and generates pressure⁴ that counteracts the gravitational pull. This causes the plasma to expand. These cycles of compression and expansion of the strongly coupled baryon-photon fluid after the Big Bang are the BAO.

There is an analogy between the dynamical effects of the BAO and the ripples on the surface of a pond emanating from falling droplets of rain. When baryons fall into the gravitational potential wells of the overdense regions of CDM, spherical compression (sound) waves in the photon-baryon fluid are generated and propagate outward. The speed of sound in the photon-baryon fluid is about half the speed of light. As noted above, the initial gravitational collapse that begins the BAO is seeded when $\delta\rho_m/\rho_m \gtrsim 1$ (where ρ_m is dominated by the CDM). This must happen relatively soon after the Big Bang, and so these initial compression waves propagate outward for $t_r \approx 400,000$ years until recombination, when atoms form and the light of the CMB is released. The largest peak in Fig. 1.3 occurs at an angular scale of $\Delta\theta \approx 1^\circ$ and $\ell \approx 220$. This feature is determined by the distance these first ripples of the BAO had travelled from the time since recombination $s \approx ct_r/2$ (the sound horizon):

$$\Delta\theta = \frac{s}{d_{\text{ls}}(z)}, \quad (1.6)$$

where $d_{\text{ls}}(z)$ is the distance to the surface of last scattering, taking into account the expansion of the universe from $z \approx 1100$.

The relationship between the angular scale of the peaks in the anisotropy of the CMB temperature fluctuations and the spatial scale of the baryon density fluctuations at recombination can be distorted by the spacetime geometry of the universe [36]. The overall spatial curvature of the universe could, in principle, be open, closed, or flat: in an open universe, initially parallel light rays would propagate along geodesics that diverge from each other; in a closed universe, initially parallel light rays would propagate along geodesics that converge; and in a flat universe (spatial curvature equals zero), initially parallel light rays would remain parallel as they propagate (geodesics are straight lines). If the spacetime geometry of the universe was open or closed, the spatial curvature would cause the observed $\Delta\theta$ and ℓ for the first peak in Fig. 1.3, corresponding to the spatial scale of the sound horizon at the surface of last scattering, to be larger or smaller than observed. The CMB measurements provide strong evidence for a flat universe (better than a part in a thousand [32–34]). The higher order peaks in Fig. 1.3 show the relative importance

⁴This pressure is what keeps the baryon-photon fluid density quite uniform in the early universe even in the presence of regions with significant CDM overdensities.

of the gravitational potential from the baryons themselves (which oscillates with the photon-baryon fluid density as it compresses and expands) as compared to the gravitational potential from the CDM which does not oscillate (due to negligible interactions, there is no dark matter “pressure” to counterbalance gravity). The ratio of dark matter density to baryon density derived from the CMB measurements is consistent with the ratio found from the velocity dispersion of galactic clusters [8], galactic rotation curves [13], and gravitational lensing studies [14, 15]. These topics are discussed in more detail in Chap. 3, Sect. 3.2.1.

There is yet another line of reasoning suggesting that a significant fraction of the mass of the universe is nonbaryonic: the primordial abundance of light elements produced by the Big Bang [37]. Early work by Gamow and Alpher [38–40]⁵ showed that light elements could be produced in the early universe via neutron capture. As the production of elements in stars and supernovae was better understood, it became apparent that, for example, deuterium (²H) in the interstellar medium could not have been produced in stars but must be a relic of the Big Bang [41]. Today, this process of Big Bang nucleosynthesis (BBN) is relatively well understood based on the Standard Model of particle physics [37].⁶ The basic concepts of BBN are described in the following tutorial.

Tutorial: Big Bang Nucleosynthesis (BBN)

A way to understand BBN is to follow particle reaction rates as the universe expands and cools after the Big Bang. Nucleosynthesis begins about ten seconds after the Big Bang. At this point in the evolution of the early universe, the energy density was dominated by relativistic species: photons, electrons, positrons, and neutrinos. Under these conditions the weak interaction rates were rapid compared to the expansion rate and established thermal and chemical equilibrium between neutron and proton densities via the reactions

$$n + e^+ \leftrightarrow p + \bar{\nu}_e ,$$

$$n + \nu_e \leftrightarrow p + e^- ,$$

$$n \leftrightarrow p + e^- + \bar{\nu}_e .$$

In equilibrium the ratio between the neutron and proton densities (n_n and n_p , respectively) is given by the Boltzmann factor

⁵ This work includes the famous “ $\alpha - \beta - \gamma$ ” paper [39] where Gamow added Hans Bethe to the author list purely for humorous purposes.

⁶ Notable exceptions to the success of the BBN model are the *lithium problems*: the observed abundance of ⁷Li is a few times smaller than the BBN predictions, and the observed abundance of ⁶Li is about three orders of magnitude higher than the BBN predictions [42].

$$\frac{n_n}{n_p} = e^{-E_{np}/k_B T}, \quad (1.7)$$

where $E_{np} = (m_n - m_p)c^2$ is the neutron-proton mass difference and T is the temperature of the universe. As the universe continued to expand and cool, eventually the weak interaction rates fell below the expansion rate, which resulted in breaking of equilibrium: the universe was expanding too fast after this point for neutrons and protons to maintain chemical equilibrium (this is known as *freeze-out*). Specifically, freeze-out occurs when the reaction rate Γ becomes smaller than the Hubble parameter H ,

$$H = \frac{\dot{a}}{a}, \quad (1.8)$$

where a is the scale factor introduced in Eqs. (1.3) and (1.4). If $\Gamma \ll H$, there is on average less than one reaction over the age of the universe ($\approx 1/H$).

The freeze-out temperature $T_f \approx 0.8 \text{ MeV}/k_B$, for which $H = \Gamma$, is predicted by the Standard Model (which describes the rates of the aforementioned weak interactions that interconvert neutrons and protons) along with general relativity and standard cosmology (which describes the expansion rate H) and gives [37]

$$\frac{n_n}{n_p} = e^{-E_{np}/k_B T_f} \approx \frac{1}{6}. \quad (1.9)$$

After freeze-out, n_n/n_p continues to decrease because of β -decay of the neutrons. The beginning of the nucleosynthesis chain with the production of deuterium (D) is delayed because of photodissociation: the ratio of the baryon density to photon density, n_B/n_γ , is so low that photodissociation of D exceeds its production. The temperature at which nucleosynthesis begins can be found by comparing the rate of D production,

$$\Gamma_{\text{prod}} \approx n_B \sigma_{\text{nc}} v, \quad (1.10)$$

to D dissociation,

$$\Gamma_{\text{dis}} \approx n_\gamma \sigma_{\text{pd}} c e^{-E_D/k_B T}, \quad (1.11)$$

where n_B and n_γ are the baryon and photon densities, respectively, σ_{nc} and σ_{pd} are the cross-sections for neutron capture and photodissociation, respectively, v is the relative velocity between baryons, and $E_D \approx 2.23 \text{ MeV}$ is the deuterium binding energy. The factor $e^{-E_D/k_B T}$ must be included in Eq. (1.11) since $n_\gamma/n_B \gg 1$ and thus $\Gamma_{\text{dis}} \gg \Gamma_{\text{prod}}$ until $k_B T \ll E_D$: there is significant photodissociation due to the high-energy tail of the thermal photon distribution.

When T becomes sufficiently low (at $k_B T \approx 0.1 \text{ MeV}$), Γ_{dis} drops below Γ_{prod} and deuterium is produced, starting the chain reaction that generates the light

elements. From this point, most of the ratios of light element abundances can be calculated from measured nuclear reaction rates and well-known Standard Model physics [37], and agree well with observations (except for ${}^6\text{Li}$ and ${}^7\text{Li}$ as mentioned in the footnote from the previous page).

End of Tutorial

The theory of BBN outlined in the above tutorial has just one free parameter: the ratio of baryon density to photon density, n_B/n_γ , at the time of when the light elements formed. Thus the measured ratios between abundances of ${}^1\text{H}$, ${}^2\text{H}$, ${}^3\text{He}$, and ${}^4\text{He}$ not only determine n_B/n_γ , but the consistency between the predicted ratios of these abundances serves as a cross-check of the theory of BBN. There is good agreement between theory and observations, validating the theory of BBN in the standard Big Bang cosmology [43, 44] and precisely measuring the baryon density produced by the Big Bang. As discussed above, from measurements of the CMB, we know that the universe has a flat spacetime geometry, which in turn implies that the total energy density measured now, $\rho_{\text{tot}}(t_0)$, is equal to the critical density, $\rho_{\text{crit}}(t_0)$, for a flat universe [45]:

$$\rho_{\text{crit}}(t_0) = \frac{3H_0^2}{8\pi G_N}, \quad (1.12)$$

where $H_0 = H(t_0)$ is the present value of the Hubble parameter. The total energy density $\rho_{\text{tot}}(t_0)$ includes contributions from both matter and an unexplained form of energy known as *dark energy*⁷ (described in the standard Big Bang cosmology by a cosmological constant Λ). The value of the dark energy density ρ_Λ can be determined from surveys of distant type Ia supernovae [51–53]. With the baryon mass density $\rho_B(t_0)$ given by measurements and calculations of the relic density of light elements [54], the density of nonbaryonic CDM can be determined:

$$\rho_{\text{CDM}}(t_0) = \frac{3H_0^2}{8\pi G_N} - \rho_B(t_0) - \rho_\Lambda(t_0). \quad (1.13)$$

The amount of dark matter found from these considerations is consistent with that found from other lines of reasoning: over 80% of the matter content of the universe is dark.

Given the diversity of evidence for dark matter outlined above, not to mention additional evidence from detailed modeling of the cosmological evolution of the universe and galaxy formation [55], is there any possibility that dark matter does

⁷ The problem of the nature of dark energy is in some ways even more perplexing than the problem of dark matter, and there may even be connections between explanations of the two phenomena [46, 47]. The interested reader is referred to Refs. [48–50] for reviews.

not exist? Historically, when the primary evidence for dark matter was derived from the rotation curves of galaxies, a plausible alternative hypothesis to explain the data was proposed by Milgrom [56, 57]: Modified Newtonian Dynamics (MOND). The main idea of MOND is that rather than introducing new particles, the laws of physics should be modified: if the nonrelativistic force due to gravity behaved as

$$F = \frac{ma^2}{a_0} \quad (1.14)$$

in the limit of very small accelerations $a \ll a_0 \approx 10^{-10} \text{ m/s}^2$, then the motion of stars in galaxies could be understood without postulating the existence of dark matter. MOND remained a viable alternative to dark matter for quite some time, but in spite of valiant attempts to extend the theory [58], MOND struggles to explain the combined observational evidence for dark matter derived from galactic clusters, gravitational lensing, CMB measurements, and BBN without, ultimately, introducing new particles [1, 59]. This is not to rule out the possibility that MOND or variants on these ideas could account for *some* of the observations described above. However, based on the multiple and distinct observations and calculations supporting the dark matter hypothesis, it is difficult to envision a scenario without some form of dark matter.

Nonetheless, one should keep in mind the complexity of the Standard Model when imagining that but a single type of particle makes up all of the dark matter: the plethora of known particles and fields in the Standard Model apparently constitute less than a fifth of the matter in the universe. Furthermore, there is always the possibility of discovering new physics that could significantly alter our understanding of the case for dark matter. For instance, a nonzero mass of the photon could partially explain the flat galactic rotation curves [60]. So while the evidence for dark matter is compelling, one should not turn a blind eye to alternative theories.

1.2 What Do (We Think) We Know About Dark Matter?

In this section we consider in turn several crucial characteristics of dark matter established by the observational evidence discussed in Sect. 1.1. Already we have seen that multiple, independent observations provide a good understanding of the total amount of mass in the form of dark matter in the universe. We also know that the dark matter must either be stable or long-lived, since the evidence shows that dark matter has been present and played a crucial role throughout the cosmological history of the universe. Furthermore, dark matter:

1. is not predominantly any of the known Standard Model particles (without the introduction of some new physics beyond the Standard Model),
2. is predominantly nonrelativistic (cold), and
3. is distributed in halos that extend well beyond the luminous matter of galaxies.

The fundamental Standard Model constituents of matter are leptons and quarks. The known stable, long-lived form of quarks are baryons: protons and bound neutrons. The preponderance of observational evidence establishes that dark matter is not made of such baryons. The baryonic content of the universe, as noted in Sect. 1.1, is determined from measurements of the CMB and the abundance of light elements produced by BBN, and establishes that dark matter cannot be ordinary baryons. The only known stable charged lepton is the electron, which when free interacts strongly with light: electrons can contribute significantly to dark matter only if they are bound to nuclei in the form of atoms, in which case the constraint on baryon density rules them out as a candidate. That leaves neutrinos.

At first glance, neutrinos appear to be an intriguing dark matter candidate: they only interact via the weak interaction (so they are indeed dark) and they are produced as a thermal relic of the Big Bang [61–63]. However, Standard Model neutrinos cannot be a substantial fraction of the dark matter for a reason related to the second item in the above list of dark matter characteristics: dark matter must be nonrelativistic (cold) rather than relativistic (hot) during the formation of structure in the early universe. This point was alluded to in the discussion of the CMB fluctuations in Sect. 1.1: only the cold dark matter (CDM) scenario can connect the measured scale of density fluctuations at recombination seen in the CMB to the observed large-scale structure of the matter in the universe in the present epoch. The random thermal motion of hot dark matter would wash out the small-scale density fluctuations needed to seed galaxy formation. When detailed cosmological models and simulations are compared to extensive surveys of the distribution of galaxies in the universe, it is clear that the observed universe matches the CDM scenario (see, for example, Refs. [64–66]).⁸

It turns out, for this reason, that Standard Model neutrinos cannot be CDM. Measurements of neutrino oscillations determine the differences between the squares of the masses of neutrino flavors: the largest square of the mass difference between neutrino flavors is $\Delta(m c^2)^2 \lesssim 2.5 \times 10^{-3} \text{ eV}^2$ [67]. Direct measurements of the electron neutrino mass from beta-decay experiments set an upper limit of $m_{\nu_e} c^2 \lesssim 2 \text{ eV}$ [68–70], proving that in fact all the Standard Model neutrinos have masses $< 10 \text{ eV}$. Neutrinos with masses $< 10 \text{ eV}$ decouple from thermal equilibrium in the early universe at a temperature where they are highly relativistic and thus cannot be CDM [63].

Furthermore, the contribution of neutrinos to the overall mass-energy density of the universe can be determined from BBN [71] and CMB measurements [32–34] and turns out to be far too small to be the dominant component of dark matter. Yet

⁸ However, it should be noted that warm dark matter, something which is relativistic but not highly relativistic, may make up some substantial fraction of the dark matter density [66].

another argument against neutrinos being the dominant contribution to dark matter⁹ (and in fact any fermion with mass below ≈ 10 eV) is considered in Problem 1.2.

? Problem 1.2 Minimum Mass of Fermionic Dark Matter

Derive a lower limit on the mass of a spin-1/2 fermionic dark matter candidate based on the facts that (a) the average mass density of dark matter in the Milky Way is $\rho_{\text{dm}} \approx 0.4 \text{ GeV/cm}^3$ [73] and (b) the escape velocity of the Milky Way galaxy is $v_{\text{esc}} \approx 2 \times 10^{-3}c$ [74].

Solution on page 305.

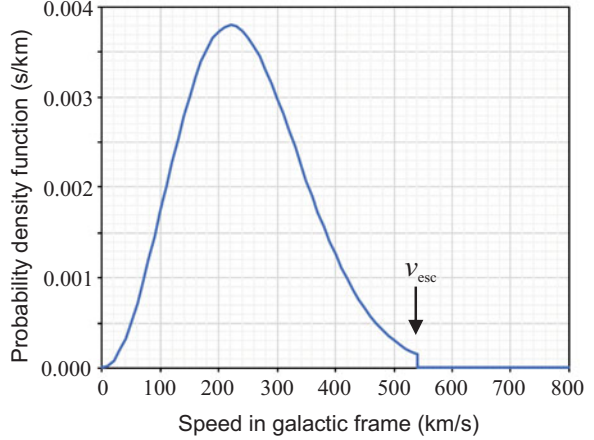
The third item on our list of dark matter characteristics concerns the distribution of dark matter in galaxies. The distribution in our own Milky Way galaxy is of particular interest for many of the experiments discussed in this text that seek to directly measure nongravitational interactions of dark matter using Earthbound detectors. As noted in Problem 1.1, dark matter must be distributed in a halo that extends far beyond the luminous matter in galaxies (about 6–8 times the distance from the galactic center as compared to luminous matter [75]). Presently, most researchers assume that the galactic dark matter distribution is described by what is known as the *standard halo model* (SHM) [76–78]. While there are certainly some notable discrepancies between the SHM’s predictions and observations [79–81], the SHM generally accounts well for galactic rotation curves within present uncertainties. Using the SHM along with observations of stars’ rotation curves in the Milky Way, a number of groups have estimated the dark matter energy density in the vicinity of our solar system to be $\rho_{\text{dm}} \approx 0.3\text{--}0.4 \text{ GeV/cm}^3$, with a model-dependent uncertainty of about a factor of two [73, 82–84]. This corresponds to a mass density equivalent to one hydrogen atom per a few cm^3 .

Dark matter particles are trapped within the gravitational potential well of the Milky Way galaxy and in the SHM are assumed to be virialized¹⁰ but not thermalized (since the absence of significant nongravitational interactions is assumed). The SHM assumes that in the galactic rest frame the velocity distribution of dark matter is isotropic with a dispersion $\Delta v \approx 290 \text{ km/s}$. The distribution of gravitationally bound dark matter in the galaxy (Fig. 1.4) naturally has a cutoff above the galactic escape velocity of $v_{\text{esc}} \approx 544 \text{ km/s}$ [74]; however, it should be noted that the speed of dark matter particles can exceed the cutoff velocity in the local vicinity of massive bodies due to gravitational acceleration, and there can also be a small fraction of

⁹ It should be noted that the argument presented in Problem 1.2 does not apply if somehow neutrinos violate the spin-statistics theorem [72], in which case they may yet be a viable dark matter candidate.

¹⁰ Although it should be recognized that there is evidence that fairly recently (within 1–2 billion years) a number of smaller galaxies have merged with the Milky Way, and the stars and dark matter from these galaxies have not had sufficient time to completely virialize [85, 86].

Fig. 1.4 Probability distribution function describing the speed of dark matter particles in the galactic frame of the Milky Way according to the SHM. There is a cutoff at the escape velocity of the galaxy ($v_{\text{esc}} \approx 544$ km/s). Figure courtesy of G. Blewitt



unbound dark matter passing through the galaxy at velocities above v_{esc} . Our solar system moves through the dark matter halo with relative velocity with respect to the galactic rest frame of ≈ 220 km/s $\approx 10^{-3}c$ toward the Cygnus constellation. It is important to note that the relative velocity of an Earthbound dark matter sensor also has both daily and seasonal modulations due to Earth’s rotation about its axis and orbit around the Sun: the Earth’s orbit creates a 10% modulation of the velocity and the Earth’s rotation can create up to a 0.2% modulation [74, 87, 88].

A final characteristic, of keen interest for the experiments discussed in this text, is the degree to which dark matter interacts nongravitationally. Some generic upper limits on the strength of interactions between dark matter and Standard Model particles and fields can be obtained from observations of the Bullet Cluster and similar galaxy cluster mergers [17], as well as measurements of galaxies and satellites of galaxies moving through dark matter halos [89] and constraints on dissipation and thermalization within dark matter halos [90]. Based on this evidence, nongravitational interactions (long-range and contact) between dark matter particles are constrained to have an average scattering-cross-section-to-mass ratio $\sigma_{\text{dm}}/m_{\text{dm}} \lesssim 0.5$ cm²/g ≈ 1 barn/GeV. This turns out to be similar to the ratio of scattering-cross-section-to-mass ratios for nuclei. Thus, generically, from astrophysical evidence it is difficult to say that the interaction strength between dark and ordinary matter is “small.” Direct experimental searches for particular classes of dark matter candidates, however, significantly constrain the interactions of such particles with Standard Model constituents [91]. It is also relevant to note that dark matter particles must be neutral (or have infinitesimal charge [92]) so that they do not interact electromagnetically (otherwise dark matter would not be dark!).

1.3 What Could Dark Matter Be?

There are a plethora of hypotheses about the nature of dark matter that span an enormous range of parameter space. For example, the masses of dark matter particle candidates range from 10^{-22} eV (fuzzy dark matter [93, 94]) up to 10^{21} eV (WIMPzillas [95]); if dark matter particles have significant self-interactions, then they can coalesce into composite objects with masses up to 10^{50} eV [96]. Several review articles explore in detail many of these hypotheses (see Refs. [83, 97–100], and, for amusement, Fig. 1.5). For brevity, here we highlight general principles and a few of the most popular hypotheses and their current experimental status.

Dark matter hypotheses regarded as “theoretically well-motivated” usually share several key attributes. The first is a plausible production mechanism that generates an abundance matching the observed dark matter density in the universe. Of course, as mentioned in Sect. 1.2, in order to match the observed density the dark matter particles must be stable: long-lived compared to the age of the universe so that they persist to the modern epoch. Another key attribute is that dark matter particles proposed in well-motivated theories also solve some other mystery of modern physics: multiple puzzles hint of their existence.

These attributes are exemplified by the hypothesis that has attracted the most attention over the last several decades: the idea that dark matter consists of *weakly interacting massive particles* (WIMPs). The WIMP hypothesis developed from the observation that particles interacting via the weak interaction would be created at just the right abundance to match the observed dark matter density [62, 102]. This is the so-called WIMP miracle. If the dark matter particles were thermally produced in the early universe, meaning that they were created in equilibrium with Standard Model particles via collisions at sufficiently high temperature, then the interaction cross-section can be estimated from arguments similar to those used to understand BBN (see the tutorial in Sect. 1.1). In the case of BBN, the

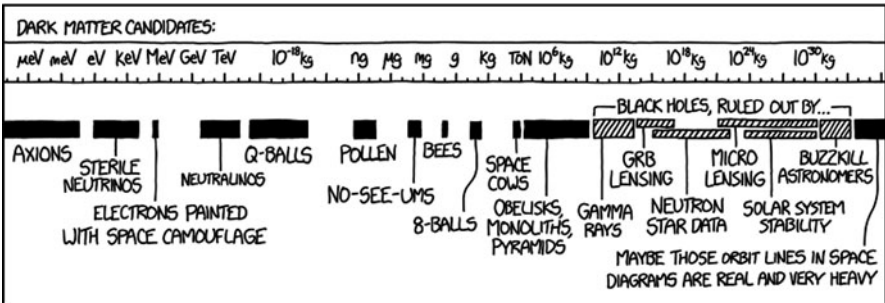


Fig. 1.5 Comical portrayal of the wide range of possible dark matter candidates and their masses from the xkcd comic strip (<https://xkcd.com/>), not too far off from the actual state of affairs at present. Actually, in some cases the cartoonist is a bit too conservative: for example, axions can have masses as small as 10^{-12} eV [100] and axionlike particles (ALPs) could have masses $\lesssim 10^{-22}$ eV [94, 101]

weak-interaction-maintained equilibrium between neutrons and protons until the universe cooled below the freeze-out temperature; analogously, there could be an interaction that maintained equilibrium between Standard Model particles (SM) and dark matter particles (χ) through a process $\chi\chi \leftrightarrow \text{SM}$ in the early universe.¹¹ As the universe continued to cool after the Big Bang, $k_B T$ would become smaller than $m_\chi c^2$, where m_χ is the dark matter particle mass, and the density n_χ would scale as $e^{-m_\chi c^2/(k_B T)}$. The decline in the dark matter density as T decreased would halt at a freeze-out temperature, leaving a relic density of dark matter—just like the relic density of baryons in the BBN scenario. This process is described by the Boltzmann equation [99]:

$$\frac{dn_\chi}{dt} = -3H_0 n_\chi - \langle \sigma_\chi v \rangle (n_\chi^2 - n_\chi(\text{eq})^2), \quad (1.15)$$

where σ_χ is the cross-section for $\chi\chi \leftrightarrow \text{SM}$, v is the relative velocity between particles, $\langle \dots \rangle$ indicates the thermal average, and $n_\chi(\text{eq})$ is the dark matter density in equilibrium. The first term on the right-hand side of Eq. (1.15) describes the decrease in dark matter density due to the expansion of the universe while the second term describes the creation and annihilation of dark matter from Standard Model particles. The solution of Eq. (1.15) yields [97–99]

$$\langle \sigma_\chi v \rangle \approx \frac{6 \times 10^{-27} \text{ cm}^3/\text{s}}{\Omega_{\text{dm}}}, \quad (1.16)$$

where $\Omega_{\text{dm}} = \rho_{\text{dm}}/\rho_{\text{crit}} \approx 0.22$ is the ratio of the dark matter density to the critical density for a flat universe. The estimate of $\langle \sigma_\chi v \rangle$ from Eq. (1.16) turns out to equal the characteristic scale of the weak interaction if $10 \text{ GeV} \lesssim m_\chi c^2 \lesssim 1 \text{ TeV}$ [99]: hence the “WIMP miracle”—weakly interacting particles can be thermally produced with a relic abundance matching the dark matter density. Furthermore, WIMPs with such masses would be nonrelativistic at the freeze-out temperature and thus would fit the CDM scenario.

It also turns out that many leading theories of physics beyond the Standard Model predict new physics at the weak interaction scale. The key motivation for these theories is the *hierarchy problem*: the mystery of why gravity is so feeble compared to the other fundamental forces of nature, the strong and electroweak interactions. In the framework of quantum field theory, the hierarchy problem can be reframed in terms of the puzzle of the smallness of the Higgs-boson mass. The Higgs mass is $m_H c^2 \approx 125 \text{ GeV}$, which can be compared to the natural mass scale of the gravitational interaction, the Planck scale:

¹¹ Notably, one of the intriguing facts about dark matter is that its density is actually quite similar to the baryon density: there is only about five times more dark matter than ordinary matter as opposed to orders of magnitude more or less, suggesting that perhaps baryons and dark matter were produced by similar processes that equilibrate their densities in the early universe.

Table 1.1 Examples of theories proposing WIMP dark matter candidates and related references

WIMP candidate	Description	References
Neutralino	Lightest superpartner in many supersymmetric models, a linear combinations of the photino, higgsino, and Z-ino.	[103, 105]
Gravitino	Superpartner of the graviton in supersymmetric models, in many scenarios only interacts gravitationally.	[106]
Little Higgs	A \approx TeV scalar WIMP predicted by an alternative to supersymmetry's solution of the hierarchy problem.	[107, 108]
Kaluza-Klein excitation	Compactified extra spatial dimensions, an ingredient of string theory, have excited modes that correspond to an infinite number of partners to standard model particles; the lightest one is a WIMP candidate.	[109, 110]

$$M_{\text{Pl}}c^2 = \sqrt{\frac{\hbar c}{G_N}} \approx 10^{19} \text{ GeV}. \quad (1.17)$$

Quantum field theory predicts that the measured (physical) Higgs mass is given by

$$m_H^2 \approx m_H(0)^2 + \Delta m_H^2, \quad (1.18)$$

where Δm_H is from radiative corrections to the “bare” mass $m_H(0)$. The natural scale of Δm_H is the energy scale at which beyond-standard-model physics appears: if there were no new physics until the Planck scale, $\Delta m_H^2 \approx M_{\text{Pl}}^2$. Unless there is a coincidental cancellation at a level of a part in 10^{34} between contributions to the radiative correction term Δm_H , the Higgs mass should be close to M_{Pl} . Since m_H is measured to be close to the weak scale, there should be beyond-standard-model physics at the weak scale in order to set $\Delta m_H c^2 \approx 100 \text{ GeV}$.

Thus, many theories proposing WIMPs share both key attributes of a well-motivated dark matter hypothesis: they give the correct dark matter abundance and also solve another mystery of modern physics, in this case the hierarchy problem.¹² Table 1.1 presents a list of some WIMP candidates and associated references.

Experiments have shown, however, that if the WIMP hypothesis is correct, the story must not be so simple. If all of dark matter consisted of particles with masses $10 \text{ GeV} \lesssim m_\chi c^2 \lesssim 1 \text{ TeV}$ that interacted with nuclei via the weak force with unsuppressed couplings, they would have been experimentally observed decades

¹² Supersymmetry [103] at the \approx TeV scale, one of the leading theories of WIMP dark matter, also predicts a unification of the electromagnetic, strong, and weak coupling constants at the “Grand Unification Theory” (GUT) scale of $\approx 10^{16} \text{ GeV}$ [104]. This is widely viewed as another tantalizing theoretical hint of WIMP dark matter.

ago. Cryogenic experiments searching for energy deposition from collisions of WIMPs with nuclei, first proposed in the 1980s [111, 112], have been pursued by a number of collaborations over the past decades. Despite several tantalizing hints of detections,¹³ ultimately none of the experiments searching for WIMPs has found evidence of WIMP dark matter. The resulting constraints from these null experiments have become increasingly stringent, ruling out many of the most attractive WIMP theories [119]. Similarly, searches for WIMP candidates at the Large Hadron Collider (LHC) have placed tight constraints on many WIMP models [120]. The situation has become increasingly dire for the WIMP hypothesis, and the motivation to explore other explanations for the nature of dark matter has become correspondingly stronger.

A hypothesis closely related to the WIMP paradigm is the suggestion that dark matter might be sterile neutrinos. Perhaps there is a heavy neutrino species that does not interact via the weak interaction but could be generated by mixing with standard model neutrinos. The sterile neutrino hypothesis possesses the key attributes of theoretically well-motivated dark matter candidate: there is a production mechanism that can give a reasonable abundance (mixing with standard model neutrinos [121]) and sterile neutrinos can also solve a number of puzzles in neutrino physics, for example, as a mechanism to generate the nonzero standard model neutrino mass [122]. Because of the mixing with standard model neutrinos, sterile neutrinos can decay into a photon and a lighter neutrino. Thus searches for x-rays from sterile neutrino decay in nearby galaxies have been able to rule out a wide region of sterile neutrino parameter space [123, 124]. Most of the rest of the sterile neutrino parameter space is ruled out by its effect on small-scale structure in the universe [125], although loopholes remain [126].

Another dark matter hypothesis that received considerable attention in the past was the possibility that dark matter consists of *massive astrophysical compact halo objects* (MACHOs): composite baryonic objects that are non-luminous, such as planets, brown dwarfs, white dwarfs, neutron stars, and black holes. The term MACHO was coined to contrast with the term WIMP, and MACHOs had the notable advantage in that they were known to exist.¹⁴ However, it turns out that MACHOs do not exist in sufficient abundance: today there is consensus that MACHOs do not constitute a large fraction of the dark matter in the universe. One of the main

¹³ The most well-known, persistent, and controversial hint of a WIMP dark matter signal comes from the DAMA/LIBRA collaboration's reports of an annually modulated rate of scattering events on top of a background [113]. WIMP scattering rates should exhibit annual modulation due to the relative motion of the Earth with respect to the dark matter halo [88], and the DAMA/LIBRA uses this annual modulation to identify possible WIMP signals. However, the measured WIMP mass and coupling constants corresponding to the DAMA/LIBRA signals have been ruled out by a number of other experiments [114, 115]. Independent experiments undertaken specifically to resolve this controversy have recently ruled out the possibility that the DAMA/LIBRA results are evidence of dark matter [116–118].

¹⁴ Along these lines, an alternative meaning of MACHO was suggested by astrophysicist Chris Stubbs: *maybe astronomy can help out!*

arguments against MACHOs as dark matter is the evidence discussed in Sects. 1.1 and 1.2 from CMB measurements and BBN that dark matter is nonbaryonic. A second argument against MACHOs as dark matter comes from gravitational microlensing studies [127]. If the dark matter halo consisted primarily of MACHOs in the mass range of $10^{-7}M_{\odot} \lesssim M \lesssim 10^2M_{\odot}$, gravitational lensing of light from visible stars by the MACHOs would cause a significant fraction of those stars (one in a million) to exhibit transient variation of their apparent brightness. Large-scale microlensing surveys have been able to constrain the contribution of MACHOs to the dark matter mass content at $\lesssim 8\%$ [127]. Importantly, these constraints apply not only to MACHOs, but also to compact objects composed of nonbaryonic matter.

It should be noted that there are special, possibly baryonic, MACHO dark matter candidates that evade the CMB and BBN bounds: primordial black holes (PBHs). In the early universe, prior to BBN, there might be regions of space with energy so dense that they gravitationally collapse into black holes [128]. This is in contrast to black holes that are later produced as the end state of stellar evolution, and hence subject to the CMB limits on baryon density at recombination and BBN limits at the time of light element formation. The PBH mass is constrained to be $\gtrsim 10^{-19}M_{\odot}$, otherwise the PBHs would have evaporated via Hawking radiation prior to the present epoch [129]. Gravitational microlensing surveys constrain the PBH mass to be $\lesssim 10^{-7}M_{\odot}$ [127].

This brings us, at last, to the dark matter hypothesis that is the subject of this book: the idea that dark matter consists primarily of ultralight bosons.

1.4 Ultralight Bosonic Dark Matter

Ultralight bosonic dark matter (UBDM) is qualitatively quite different from the dark matter particles considered in Sect. 1.3. WIMPs and sterile neutrinos are particles with masses $\gg 10$ eV and the search methods are aimed at detecting individual interactions of dark matter particles. In contrast, UBDM consists of bosons with masses $\ll 10$ eV (hence *ultralight*) and the search methods are aimed at detecting coherent effects of UBDM waves. This difference in search methodologies arises from the fact that in order to match the observed dark matter density, the mode occupation number of the ultralight bosons can be quite high (Problem 1.3). In this case it is natural to treat UBDM as a classical field and take advantage of its coherent wavelike properties. A useful analogy can be made with radio waves: an efficient method of detection is to measure the electron current coherently driven by the radio waves using an antenna, as opposed to detecting single photons.

? Problem 1.3 Ultralight Bosonic Dark Matter Waves

Suppose that dark matter consists mostly of bosons with mass $m_b c^2 = 10^{-6}$ eV. What are the Compton frequency and Compton wavelength of such bosons? Recalling that the virialized velocity of dark matter in the Milky Way is $\approx 10^{-3}c$,

what is the de Broglie wavelength λ_{dB} of such bosons? Given that the local dark matter density is $\rho_{\text{dm}} \approx 0.4 \text{ GeV/cm}^3$, estimate how many bosons occupy a volume corresponding to λ_{dB}^3 ? Repeat these estimates for dark matter bosons with mass $m_b c^2 = 10^{-12} \text{ eV}$.

Solution on page 307.

In the rest frame of the UBDM, the oscillation frequency of the UBDM field is given by the Compton frequency,

$$\omega_c = \frac{mc^2}{\hbar}. \quad (1.19)$$

Of course, as noted in Sect. 1.2, in the SHM the dark matter particles are assumed to be virialized in the gravitational potential well of the galaxy. This leads to a random distribution of boson velocities. In the Milky Way, the characteristic width of the distribution is $\Delta v \approx 10^{-3}c$, about equal to the velocity of our solar system relative to the galactic rest frame. The spread in boson velocities gives rise to frequency dispersion, since an observable UBDM field arises from interference between a multitude of bosons with different velocities. Therefore an UBDM field has a characteristic coherence time τ_{coh} and coherence length L_{coh} , as considered in Problem 1.4.

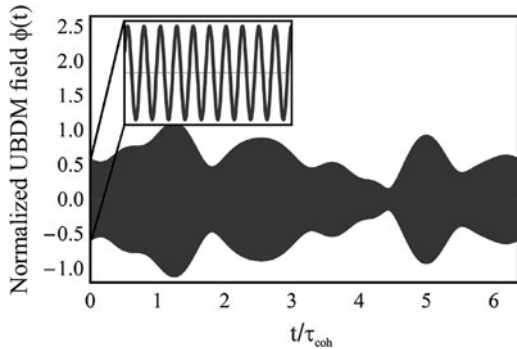
? Problem 1.4 Coherence of Ultralight Bosonic Dark Matter Fields

Given that the characteristic width of the UBDM velocity distribution in the Milky Way is $\Delta v \approx 10^{-3}c$, derive τ_{coh} and L_{coh} for the UBDM field. Carry out numerical estimates of τ_{coh} and L_{coh} for the boson masses considered in Problem 1.3 ($m_b c^2 = 10^{-6} \text{ eV}$ and $m_b c^2 = 10^{-12} \text{ eV}$). What would be the corresponding Q -factor for the UBDM in the Milky Way, $Q = \omega/\Delta\omega$?

Solution on page 308.

Since, if we assume UBDM is described by the SHM, the observable UBDM field is the result of the interference of bosons with random velocities, its properties undergo stochastic variation with characteristic time scale τ_{coh} and length scale L_{coh} . Figure 1.6 shows a simulated virialized UBDM field over several coherence times. The amplitude of the UBDM field, while relatively constant over time durations $\Delta t \ll \tau_{\text{coh}}$, varies randomly on longer time scales. In fact, the stochastically varying amplitude of a virialized UBDM field is described by the Rayleigh distribution, which also describes the statistical properties of thermal (chaotic) light. As long as an experiment measures the UBDM field for a time $\Delta t \gg \tau_{\text{coh}}$, the experimental results can be interpreted based on the average dark matter properties. However, for

Fig. 1.6 Simulated virialized UBDM field $\phi(t)$. The inset shows the coherent oscillations of the UBDM field over a time scale $\ll \tau_{\text{coh}}$



extremely low-mass bosons it is impractical to measure for a time longer than τ_{coh} . For example, fuzzy dark matter [93, 94] with boson mass $m_b c^2 \approx 10^{-22}$ eV would have $\tau_{\text{coh}} \approx 4 \times 10^{13}$ s (roughly a million years!). In such cases, the interpretation of experiments must take into account the stochastic nature of UBDM [130].

It should be noted that the distribution of UBDM in the Milky Way may deviate from the predictions of the SHM in various ways. There can be enhancement (or suppression) of the local dark matter density due to formation of “clumps” or streams [131]. A related possibility is that self-interactions or topological properties of the UBDM field could lead to the formation of large composite structures such as condensates [132], clusters [133], boson stars [134], or domain walls [135, 136]. A reasonable assumption is that the motion and distribution of such composite structures are described by the SHM. On the other hand, some fraction of the UBDM could become trapped in the local gravitational potential of the Earth or Sun [137], creating a local halo where the UBDM density is enhanced. The fact that much is unknown about the local dark matter density should be taken into account when interpreting terrestrial experiments searching for UBDM.

One of the most well-motivated UBDM candidates from the perspective of theory, according to the criteria developed in Sect. 1.3, is the *axion* [138, 139]. The existence of axions is predicted by a proposal to solve the so-called *strong-CP problem*. *CP* refers to the combined symmetry with respect to charge-conjugation (*C*), transformation between matter and anti-matter, and spatial inversion, i.e., parity (*P*).¹⁵ The strong *CP* problem arises from a *CP*-violating term appearing in the Lagrangian describing quantum chromodynamics (QCD) [140, 141]. The magnitude of *CP* violation in the strong interaction caused by this term is governed by a phase $\bar{\theta}_{\text{QCD}}$. Experimentally, $\bar{\theta}_{\text{QCD}}$ is found to be vanishingly small: constraints on the neutron electric dipole moment (EDM) imply that $\bar{\theta}_{\text{QCD}} \lesssim 10^{-10}$ [142]. This creates a so-called *fine-tuning problem*, since $\bar{\theta}_{\text{QCD}}$ is an arbitrary phase in QCD that could, in principle, take on any value from zero to 2π : the fact that $\bar{\theta}_{\text{QCD}}$ is near zero seems to be an unlikely coincidence. A solution to the strong *CP* problem

¹⁵ A *P*-invariant interaction is said to possess *chiral symmetry*.

was proposed by Roberto Peccei and Helen Quinn [143, 144]: perhaps $\bar{\theta}_{\text{QCD}}$ does not possess a constant value, but rather evolves dynamically and naturally tends to a value near zero due to spontaneous symmetry breaking (see Ref. [145] for an intuitive explanation).¹⁶ In this model, the CP -violating $\bar{\theta}_{\text{QCD}}$ term is replaced by a term in the QCD Lagrangian representing a dynamical field, and the quantum of this field is a spin-0 particle known as the axion. Furthermore, there are a number of plausible mechanisms to generate axions matching the observed abundance of dark matter [146–151], and such axions naturally fit the CDM paradigm [100, 152] (although, it is important to note as discussed in Chap. 3, Sect. 3.2, the CDM and UBDM scenarios are not entirely equivalent and can, in principle, be distinguished). The axion mass m_a is quite small: upper limits based on astrophysical observations are $m_a c^2 \lesssim 10 \text{ meV}$ [153], and in principle m_a can be smaller than 10^{-12} eV [154].

Independent of the strong CP problem, ultralight spin-0 bosons are ubiquitous features of many theories of physics beyond the Standard Model. For example, axionlike particles (ALPs) appear in theories with spontaneous breaking of flavor symmetry (familons [155, 156]), models with spontaneous breaking of chiral lepton symmetry (arions [157]), and versions of quantum gravity (spin-0 gravitons [158–161]). Axions and ALPs also generically arise in string theory as excitations of quantum fields that extend into extra compactified spacetime dimensions [162], with masses ranging all the way to $m_a c^2 \approx 10^{-33} \text{ eV}$ [101]. Another ALP, known as the relaxion, has been proposed to solve the hierarchy problem [163]. Axions and ALPs have also been shown to offer a plausible mechanism to generate the matter-antimatter asymmetry of the universe [164, 165].

The characteristic amplitude of the axion dark matter field is estimated in Problem 1.5.

? Problem 1.5 Axion Dark Matter Field Amplitude

Based on the fact that the axion field φ is described (ignoring self-interactions) by the Lagrangian

$$\mathcal{L} = \frac{1}{2}(\partial_\mu \varphi)\partial^\mu \varphi - \frac{1}{2}\left(\frac{m_a c}{\hbar}\right)^2 \varphi^2, \quad (1.20)$$

where ∂_μ denotes the four-derivative and \mathcal{L} has units of energy density, what are the units of φ ? What is the relationship between the time-averaged value of the square of the axion field $\langle \varphi^2 \rangle$ and the average dark matter density in the galaxy ρ_{dm} ?

Solution on page 308.

¹⁶ The underlying physics of the Peccei-Quinn solution to the strong CP problem is closely related to the physics behind the Higgs mechanism endowing particles with mass in the Standard Model.

Axions are also involved in a rather different CDM theoretical framework (see [166, 167] and the references therein) that appears to be able to account for the origin of dark matter and also explain a number of other puzzles, including the baryon asymmetry of the Universe, the roughly similar abundance of luminous and dark matter, the lithium anomalies in the BBN [168], etc. In this model, dark matter consists of “nuggets” of some 10^{25} quarks at roughly the nuclear density held together by an “axion domain wall.” The axion-quark-nugget model assumes the existence of both nuggets containing quarks and “anti-nuggets” containing antiquarks, such that the total number of quarks and antiquarks in the universe is roughly the same, thus resolving the mystery of the matter-antimatter asymmetry. The axion-quark nugget radius is on the order of 10^{-5} cm and, in contrast to most other dark matter scenarios, the interactions of such a nugget with normal matter are not feeble. For example, the cross-section for proton annihilation is on the order of the geometrical cross-section of 3×10^{-10} cm². The reason such nuggets are “dark” is that they have an unusually small cross-section-to-mass ratio.

Spin-1 bosons form another class of UBDM candidates. There are twelve fundamental spin-1 bosons in the Standard Model: the photon, the W^\pm and Z bosons, and the eight gluons. Generally speaking, a massless spin-1 boson appears for any unbroken $\mathbb{U}(1)$ gauge symmetry.¹⁷ New massless spin-1 bosons are referred to as paraxions γ' [170] in analogy with photons, the quanta arising from the $\mathbb{U}(1)$ gauge symmetry of electromagnetism. Of interest as dark matter candidates are exotic spin-1 bosons that possess nonzero mass, as does the Z boson in the Standard Model. A nonzero mass for such a hypothetical Z' boson could arise from the breaking of a new $\mathbb{U}(1)$ gauge symmetry. There are a plethora of theoretical models predicting new Z' bosons and theoretically motivated masses and couplings to quarks and leptons extend over a broad range [171]. Z' bosons that do not directly interact with Standard Model particles (and therefore reside in the so-called hidden sector) are commonly referred to as *hidden photons* [170]. Like axions and ALPs, ultralight spin-1 bosons could plausibly be produced with the correct abundance to be the dark matter [172–174]. The characteristic magnitudes of the hidden electric and magnetic fields are estimated in Problem 1.6.

? Problem 1.6 Dark Electromagnetic Fields

Equating the average dark matter density ρ_{dm} to the energy density in the hidden electric field \mathcal{E}' (given by an analog to standard electromagnetism) yields:

$$\rho_{\text{dm}} \approx \frac{1}{8\pi} (\mathcal{E}')^2. \quad (1.21)$$

¹⁷ Such symmetries arise quite naturally, for example, in string theory [169] and other Standard Model extensions. $\mathbb{U}(1)$ refers to the unitary group of degree 1, the collection of all complex numbers with absolute value 1 under multiplication.

Because the hidden photons have nonzero mass, there is a rest frame of the hidden photons for which there is only a hidden electric field oscillating at the Compton frequency. The hidden magnetic field is given by the relativistic transform of \mathcal{E}' when there is relative motion between an observer and the hidden photons

$$\mathcal{B}' \approx \frac{v}{c} \mathcal{E}' . \quad (1.22)$$

Using Eqs. (1.21) and (1.22), the local dark matter density $\rho_{\text{dm}} \approx 0.4 \text{ GeV/cm}^3$, and the characteristic relative velocity of Earth with respect to the dark matter halo of $v \approx 10^{-3}c$, estimate \mathcal{E}' and \mathcal{B}' .

Solution on page 309.

Ultralight bosons can couple to Standard Model particles and fields through a number of distinct *portals* [175] as discussed in Chap. 2. A spin-0 bosonic field φ can directly couple to fermions in two possible ways: through a *scalar* vertex or through a *pseudoscalar* vertex [176–178]. In the nonrelativistic limit (small fermion velocity and momentum transfer), a fermion coupling to φ via a scalar vertex acts as a monopole and a fermion coupling to φ via a pseudoscalar vertex acts as a dipole. This can be understood from the fact that in the particle’s center of mass frame, there are only two vectors from which to form a scalar/pseudoscalar quantity: the spin \mathbf{s} and the momentum \mathbf{p} (since the field φ is a scalar), so either the vertex does not involve \mathbf{s} (monopole coupling) or if it does, it depends on $\mathbf{s} \cdot \mathbf{p}$, which is a P -odd, pseudoscalar term. Hence the pseudoscalar interaction of φ is the source of new dipole interactions that are manifest as spin-dependent energy shifts. The scalar interaction gives rise to apparent variations of fundamental constants [175]. Spin-0 fields can also couple to the electromagnetic field:¹⁸ a number of experiments exploit this coupling to search for conversion of axions into photons in strong magnetic fields. As suggested by the original theoretical motivation for the axion, the Peccei-Quinn solution of the strong CP problem [143, 144], axions couple to the gluon field and can generate EDMs along the spin direction [182]. Analogously to photons, spin-1 bosons can generate spin-dependent energy shifts and can also mix with the electromagnetic field [175]. These distinct portals for observing the effects of UBDM offer a variety of possibilities for direct detection, discussed in detail in the subsequent chapters of this book.

¹⁸ In general, pseudoscalar particles such as axions can be produced by the interaction of two photons via a process known as the Primakoff effect [179] (discussed in Chaps. 2–5), and consequently an axion interacting with an electromagnetic field can produce a photon via the inverse Primakoff effect [180]; see also the review [181].

1.5 Conclusion

There is a strong case for the existence of dark matter: multiple independent astrophysical observations point to a consistent model where over 80% of the matter in the universe is dark. But the fundamental nature of dark matter is a complete mystery. A wide range of theories of physics beyond the Standard Model suggest there may exist heretofore undiscovered ultralight bosons with the right characteristics to explain the mystery of dark matter. In the following chapters, the rich and interesting physics of UBDM and the diverse array of experiments searching for evidence of its existence are explored.

Acknowledgments We are grateful to Alex Sushkov, Arne Wickenbrock, Alex Gramolin, Gary Centers, Peter Graham, Surjeet Rajendran, Maxim Pospelov, Andrei Derevianko, Victor Flambaum, Mikhail Kozlov, Gilad Perez, and Ariel Zhitnitsky for helpful discussions.

References

1. G. Bertone, D. Hooper, *Rev. Mod. Phys.* **90**, 045002 (2018)
2. E. Öpik, *Bull. de la Soc. Astr. de Russie* **21**, 5 (1915)
3. J.H. Oort et al., *Bull. Astron. Inst. Neth.* **6**, 249 (1932)
4. F. Zwicky, *Helv. Phys. Acta* **6**, 138 (1933)
5. F. Zwicky, *Astrophys. J.* **86**, 217 (1937)
6. A. Vikhlinin, A. Kravtsov, W. Forman, C. Jones, M. Markevitch, S. Murray, L. Van Speybroeck, *Astrophys. J.* **640**, 691 (2006)
7. L.P. David, C. Jones, W. Forman, *Astrophys. J.* **748**, 120 (2012)
8. R.W. Schmidt, S. Allen, *Mon. Not. Roy. Astron. Soc.* **379**, 209 (2007)
9. V.C. Rubin, W.K. Ford Jr, *Astrophys. J.* **159**, 379 (1970)
10. D. Rogstad, G. Shostak, *Astrophys. J.* **176**, 315 (1972)
11. R.N. Whitehurst, M.S. Roberts, *Astrophys. J.* **175**, 347 (1972)
12. M. Roberts, A. Rots, *Astron. Astrophys.* **26**, 483 (1973)
13. V.C. Rubin, W.K. Ford Jr, N. Thonnard, *Astrophys. J.* **225**, L107 (1978)
14. M. Bartelmann, *Classical Quantum Gravity* **27**, 233001 (2010)
15. H. Hoekstra, M. Bartelmann, H. Dahle, H. Israel, M. Limousin, M. Meneghetti, *Space Sci. Rev.* **177**, 75 (2013)
16. D. Clowe, M. Bradač, A.H. Gonzalez, M. Markevitch, S.W. Randall, C. Jones, D. Zaritsky, *Astrophys. J. Lett.* **648**, L109 (2006)
17. D. Harvey, R. Massey, T. Kitching, A. Taylor, E. Tittley, *Science* **347**, 1462 (2015)
18. C. Hernández-Monteagudo, J. Rubiño-Martín, R. Sunyaev, *Mon. Not. Roy. Astron. Soc.* **380**, 1656 (2007)
19. A. Lewis, *J. Cosm. Astropart. Phys.* **2013**, 053 (2013)
20. P.J. Peebles, J. Yu, *Astrophys. J.* **162**, 815 (1970)
21. R.A. Sunyaev, Y.B. Zeldovich, *Astrophys. Space Sci.* **7**, 3 (1970)
22. A. Doroshkevich, Y.B. Zel'dovich, R. Sunyaev, *Sov. Astron.* **22**, 523 (1978)
23. T. Padmanabhan, *Structure Formation in the Universe* (Cambridge University Press, Cambridge, 1993)

24. P.J.E. Peebles, *Principles of Physical Cosmology* (Princeton University Press, Princeton, 1993)
25. S. Weinberg, *Cosmology* (Oxford University Press, Oxford, 2008)
26. L. Anderson, E. Aubourg, S. Bailey, D. Bizyaev, M. Blanton, A.S. Bolton, J. Brinkmann, J.R. Brownstein, A. Burden, A.J. Cuesta et al., *Mon. Not. Roy. Astron. Soc.* **427**, 3435 (2012)
27. R.S. Ellis, R.J. McLure, J.S. Dunlop, B.E. Robertson, Y. Ono, M.A. Schenker, A. Koekemoer, R.A. Bowler, M. Ouchi, A.B. Rogers et al., *Astrophys. J. Lett.* **763**, L7 (2012)
28. G.R. Blumenthal, S. Faber, J.R. Primack, M.J. Rees, *Nature* **311**, 517 (1984)
29. P. Peebles, *Astrophys. J.* **263**, L1 (1982)
30. D.J. Eisenstein, W. Hu, *Astrophys. J.* **496**, 605 (1998)
31. A. Meiksin, M. White, J. Peacock, *Mon. Not. Roy. Astron. Soc.* **304**, 851 (1999)
32. C.L. Bennett, D. Larson, J. Weiland, N. Jarosik, G. Hinshaw, N. Odegard, K. Smith, R. Hill, B. Gold, M. Halpern et al., *Astrophys. J. Suppl.* **208**, 20 (2013)
33. P.A. Ade, N. Aghanim, M. Arnaud, M. Ashdown, J. Aumont, C. Baccigalupi, A. Banday, R. Barreiro, J. Bartlett, N. Bartolo et al., *Astron. Astrophys.* **594**, A13 (2016)
34. G. Hinshaw, D. Larson, E. Komatsu, D.N. Spergel, C. Bennett, J. Dunkley, M. Nolta, M. Halpern, R. Hill, N. Odegard et al., *Astrophys. J. Suppl.* **208**, 19 (2013)
35. P. Gorenstein, W. Tucker, *Adv. High Energy Phys.* **2014** (2014)
36. W. Hu, S. Dodelson, *Ann. Rev. Astron. Astrophys.* **40**, 171 (2002)
37. B.D. Fields, K.A. Olive, *Nucl. Phys. A* **777**, 208 (2006)
38. G. Gamow, *Phys. Rev.* **70**, 572 (1946)
39. R.A. Alpher, H. Bethe, G. Gamow, *Phys. Rev.* **73**, 803 (1948)
40. R.A. Alpher, J.W. Follin Jr, R.C. Herman, *Phys. Rev.* **92**, 1347 (1953)
41. H. Reeves, J. Audouze, W.A. Fowler, D.N. Schramm, *The Big Bang and Other Explosions in Nuclear and Particle Astrophysics*, vol. 179 (World Scientific, Singapore, 1996), pp. 65–86
42. B.D. Fields, *Ann. Rev. Nucl. Part. Sci.* **61**, 47 (2011)
43. T.P. Walker, G. Steigman, D.N. Schramm, K.A. Olive, H.S. Kang, *The Big Bang and Other Explosions in Nuclear and Particle Astrophysics* (World Scientific, Singapore, 1991), pp. 43–61
44. K.A. Olive, G. Steigman, T.P. Walker, *Phys. Rep.* **333**, 389 (2000)
45. L. Bergström, *Phys. Scr.* **2013**, 014014 (2013)
46. T. Padmanabhan, T.R. Choudhury, *Phys. Rev. D* **66**, 081301 (2002)
47. E.P. Verlinde, *SciPost Phys.* **2**, 016 (2017)
48. M. Tanabashi, K. Hagiwara, K. Hikasa, K. Nakamura, Y. Sumino, F. Takahashi, J. Tanaka, K. Agashe, G. Aielli, C. Amsler et al., *Phys. Rev. D* **98**, 030001 (2018)
49. P.J.E. Peebles, B. Ratra, *Rev. Mod. Phys.* **75**, 559 (2003)
50. L. Amendola, S. Tsujikawa, *Dark Energy: Theory and Observations* (Cambridge University Press, Cambridge, 2010)
51. A.G. Riess, A.V. Filippenko, P. Challis, A. Clocchiatti, A. Diercks, P.M. Garnavich, R.L. Gilliland, C.J. Hogan, S. Jha, R.P. Kirshner et al., *Astron. J.* **116**, 1009 (1998)
52. S. Perlmutter, G. Aldering, G. Goldhaber, R. Knop, P. Nugent, P. Castro, S. Deustua, S. Fabbro, A. Goobar, D. Groom et al., *Astrophys. J.* **517**, 565 (1999)
53. D. Scolnic, D. Jones, A. Rest, Y. Pan, R. Chornock, R. Foley, M. Huber, R. Kessler, G. Narayan, A. Riess et al., *Astrophys. J.* **859**, 101 (2018)
54. S. Burles, K.M. Nollett, M.S. Turner, *Astrophys. J. Lett.* **552**, L1 (2001)
55. J. Schaye, R.A. Crain, R.G. Bower, M. Furlong, M. Schaller, T. Theuns, C. Dalla Vecchia, C.S. Frenk, I. McCarthy, J.C. Helly et al., *Mon. Not. Roy. Astron. Soc.* **446**, 521 (2014)
56. M. Milgrom, *Astrophys. J.* **270**, 365 (1983)
57. M. Milgrom, *Astrophys. J.* **302**, 617 (1986)
58. J.D. Bekenstein, *Phys. Rev. D* **70**, 083509 (2004)
59. B. Famaey, S.S. McGaugh, *Living Rev. Relativ.* **15**, 10 (2012)
60. D.D. Ryutov, D. Budker, V.V. Flambaum, *Astrophys. J.* **871**, 218 (2019)

61. S. Gershtein, Y.B. Zel'dovich, JETP Lett. **4**, 1 (1966)
62. Y.B. Zel'dovich, A. Klypin, M.Y. Khlopov, V. Chechetkin, Sov. J. Nucl. Phys. **31**, 664 (1980)
63. S.D. White, C. Frenk, M. Davis, Astrophys. J. **274**, L1 (1983)
64. U. Seljak, A. Makarov, P. McDonald, H. Trac, Phys. Rev. Lett. **97**, 191303 (2006)
65. M. Vogelsberger, S. Genel, V. Springel, P. Torrey, D. Sijacki, D. Xu, G. Snyder, S. Bird, D. Nelson, L. Hernquist, Nature **509**, 177 (2014)
66. P. Bode, J.P. Ostriker, N. Turok, Astrophys. J. **556**, 93 (2001)
67. D. Forero, M. Tortola, J. Valle, Phys. Rev. D **90**, 093006 (2014)
68. C. Kraus, B. Bornschein, L. Bornschein, J. Bonn, B. Flatt, A. Kovalik, B. Ostrick, E. Otten, J. Schall, T. Thümmel et al., Eur. Phys. J. C **40**, 447 (2005)
69. E. Otten, C. Weinheimer, Rep. Prog. Phys. **71**, 086201 (2008)
70. V. Aseev, A. Belesev, A. Berlev, E. Geraskin, A. Golubev, N. Likhovid, V. Lobashev, A. Nozik, V. Pantuev, V. Parfenov et al., Phys. Rev. D **84**, 112003 (2011)
71. R.H. Cyburt, B.D. Fields, K.A. Olive, E. Skillman, Astropart. Phys. **23**, 313 (2005)
72. A. Dolgov, A.Y. Smirnov, Phys. Lett. B **621**, 1 (2005)
73. J. Bovy, S. Tremaine, Astrophys. J. **756**, 89 (2012)
74. K. Freese, M. Lisanti, C. Savage, Rev. Mod. Phys. **85**, 1561 (2013)
75. J. Diemand, M. Kuhlen, P. Madau, Astrophys. J. **657**, 262 (2007)
76. J. Dubinski, R. Carlberg, Astrophys. J. **378**, 496 (1991)
77. J.F. Navarro, in *Symposium: International Astronomical Union*, vol. 171 (Cambridge University Press, Cambridge, 1996), pp. 255–258
78. P. Salucci, A. Borriello, in *Particle Physics in the New Millennium* (Springer, Berlin, 2003), pp. 66–77
79. A. Klypin, A.V. Kravtsov, O. Valenzuela, F. Prada, Astrophys. J. **522**, 82 (1999)
80. B. Moore, S. Ghigna, F. Governato, G. Lake, T. Quinn, J. Stadel, P. Tozzi, Astrophys. J. Lett. **524**, L19 (1999)
81. M. Boylan-Kolchin, J.S. Bullock, M. Kaplinghat, Mon. Not. Roy. Astron. Soc.: Lett. **415**, L40 (2011)
82. L. Bergström, P. Ullio, J.H. Buckley, Astropart. Phys. **9**, 137 (1998)
83. G. Bertone, D. Hooper, J. Silk, Phys. Rep. **405**, 279 (2005)
84. M. Kamionkowski, S.M. Koushiappas, Phys. Rev. D **77**, 103509 (2008)
85. M. Lisanti, D.N. Spergel, Phys. Dark Universe **1**, 155 (2012)
86. C.A.J. O'Hare, C. McCabe, N.W. Evans, G. Myeong, V. Belokurov, Phys. Rev. D **98**, 103006 (2018)
87. A. Bandyopadhyay, D. Majumdar, Astrophys. J. **746**, 107 (2012)
88. A.K. Drukier, K. Freese, D.N. Spergel, Phys. Rev. D **33**, 3495 (1986)
89. F. Kahlhoefer, K. Schmidt-Hoberg, M.T. Frandsen, S. Sarkar, Mon. Not. Roy. Astron. Soc. **437**, 2865 (2013)
90. O.Y. Gnedin, J.P. Ostriker, Astrophys. J. **561**, 61 (2001)
91. D.S. Akerib, H. Araújo, X. Bai, A. Bailey, J. Balajthy, S. Bedikian, E. Bernard, A. Bernstein, A. Bolozdynya, A. Bradley et al., Phys. Rev. Lett. **112**, 091303 (2014)
92. J.M. Cline, Z. Liu, W. Xue, Phys. Rev. D **85**, 101302 (2012)
93. W. Hu, R. Barkana, A. Gruzinov, Phys. Rev. Lett. **85**, 1158 (2000)
94. L. Hui, J.P. Ostriker, S. Tremaine, E. Witten, Phys. Rev. D **95**, 043541 (2017)
95. D.J. Chung, E.W. Kolb, A. Riotto, Phys. Rev. D **59**, 023501 (1998)
96. D.M. Grabowska, T. Melia, S. Rajendran, Phys. Rev. D **98**, 115020 (2018)
97. G. Bertone, *Particle Dark Matter: Observations, Models and Searches* (Cambridge University Press, Cambridge, 2010)
98. L.E. Strigari, Phys. Rep. **531**, 1 (2013)
99. J.L. Feng, Ann. Rev. Astron. Astrophys. **48**, 495 (2010)
100. P.W. Graham, I.G. Irastorza, S.K. Lamoreaux, A. Lindner, K.A. van Bibber, Ann. Rev. Nucl. Part. Sci. **65**, 485 (2015)

101. A. Arvanitaki, S. Dimopoulos, S. Dubovsky, N. Kaloper, J. March-Russell, *Phys. Rev. D* **81**, 123530 (2010)
102. B.W. Lee, S. Weinberg, *Phys. Rev. Lett.* **39**, 165 (1977)
103. G. Jungman, M. Kamionkowski, K. Griest, *Phys. Rep.* **267**, 195 (1996)
104. U. Amaldi, W. de Boer, H. Fürstenau, *Phys. Lett. B* **260**, 447 (1991)
105. H. Goldberg, *Phys. Rev. Lett.* **50**, 1419 (1983)
106. J.L. Feng, A. Rajaraman, F. Takayama, *Phys. Rev. Lett.* **91**, 011302 (2003)
107. A. Birkedal, A. Noble, M. Perelstein, A. Spray, *Phys. Rev. D* **74**, 035002 (2006)
108. H.C. Cheng, I. Low, *J. High Energy Phys.* **2003**, 051 (2003)
109. H.C. Cheng, J.L. Feng, K.T. Matchev, *Phys. Rev. Lett.* **89**, 211301 (2002)
110. K. Kong, K.T. Matchev, *J. High Energy Phys.* **2006**, 038 (2006)
111. A. Drukier, L. Stodolsky, *Phys. Rev. D* **30**, 2295 (1984)
112. M.W. Goodman, E. Witten, *Phys. Rev. D* **31**, 3059 (1985)
113. R. Bernabei, P. Belli, F. Cappella, R. Cerulli, C. Dai, A. d'Angelo, H. He, A. Incicchitti, H. Kuang, X. Ma et al., *Eur. Phys. J. C* **67**, 39 (2010)
114. R. Agnese, T. Aramaki, I. Arnquist, W. Baker, D. Balakishiyeva, S. Banik, D. Barker, R.B. Thakur, D. Bauer, T. Binder et al., *Phys. Rev. Lett.* **120**, 061802 (2018)
115. A. Tan, X. Xiao, X. Cui, X. Chen, Y. Chen, D. Fang, C. Fu, K. Giboni, F. Giuliani, H. Gong et al., *Phys. Rev. D* **93**, 122009 (2016)
116. G. Adhikari et al., *Nature* **564**, 83 (2018)
117. G. Adhikari, P. Adhikari, E.B. de Souza, N. Carlin, S. Choi, M. Djamel, A. Ezeribe, C. Ha, I. Hahn, E. Jeon et al., *Phys. Rev. Lett.* **123**, 031302 (2019)
118. G. Adhikari, E.B. de Souza, N. Carlin, J. Choi, S. Choi, M. Djamel, A. Ezeribe, L. França, C. Ha, I. Hahn et al., *Sci. Adv.* **7**, eabk2699 (2021)
119. L. Roszkowski, E.M. Sessolo, S. Trojanowski, *Rep. Prog. Phys.* **81**, 066201 (2018)
120. G. Bertone, N. Bozorgnia, J.S. Kim, S. Liem, C. McCabe, S. Otten, R.R. de Austri, J. Cosm. Astropart. Phys. **2018**, 026 (2018)
121. S. Dodelson, L.M. Widrow, *Phys. Rev. Lett.* **72**, 17 (1994)
122. L. Canetti, M. Drewes, M. Shaposhnikov, *Phys. Rev. Lett.* **110**, 061801 (2013)
123. M. Viel, J. Lesgourgues, M.G. Haehnelt, S. Matarrese, A. Riotto, *Phys. Rev. D* **71**, 063534 (2005)
124. U. Seljak, A. Slosar, P. McDonald, *J. Cosm. Astropart. Phys.* **2006**, 014 (2006)
125. K. Abazajian, S.M. Koushiappas, *Phys. Rev. D* **74**, 023527 (2006)
126. X. Shi, G.M. Fuller, *Phys. Rev. Lett.* **82**, 2832 (1999)
127. P. Tisserand, L. Le Guillou, C. Afonso, J. Albert, J. Andersen, R. Ansari, É. Aubourg, P. Bareyre, J. Beaulieu, X. Charlot et al., *Astron. Astrophys.* **469**, 387 (2007)
128. B.J. Carr, S.W. Hawking, *Mon. Not. Roy. Astron. Soc.* **168**, 399 (1974)
129. A.S. Josan, A.M. Green, K.A. Malik, *Phys. Rev. D* **79**, 103520 (2009)
130. G.P. Centers, J.W. Blanchard, J. Conrad, N.L. Figueroa, A. Garcon, A.V. Gramolin, D.F. Jackson Kimball, M. Lawson, B. Pelssers, J.A. Smiga et al., *Nature Comm.* **12**, 7321 (2021)
131. J. Diemand, M. Kuhlen, P. Madau, M. Zemp, B. Moore, D. Potter, J. Stadel, *Nature* **454**, 735 (2008)
132. P. Sikivie, Q. Yang, *Phys. Rev. Lett.* **103**, 111301 (2009)
133. E.W. Kolb, I.I. Tkachev, *Phys. Rev. Lett.* **71**, 3051 (1993)
134. D. Jackson Kimball, D. Budker, J. Eby, M. Pospelov, S. Pustelny, T. Scholtes, Y. Stadnik, A. Weis, A. Wickenbrock, *Phys. Rev. D* **97**, 043002 (2018)
135. M. Pospelov, S. Pustelny, M.P. Ledbetter, D.F. Jackson Kimball, W. Gawlik, D. Budker, *Phys. Rev. Lett.* **110**, 021803 (2013)
136. A. Derevianko, M. Pospelov, *Nature Phys.* **10**, 933 (2014)
137. A. Banerjee, D. Budker, J. Eby, H. Kim, G. Perez, *Commun. Phys.* **3**, 1 (2020)
138. K. van Bibber, L.J. Rosenberg, *Phys. Today* **59**, 30 (2006)

139. K. van Bibber, K. Lehnert, A. Chou, *Phys. Today* **72**, 48 (2019)
140. R. Peccei, *Lect. Notes Phys.* **741**, 3 (2008)
141. J.E. Kim, G. Carosi, *Rev. Mod. Phys.* **82**, 557 (2010)
142. C.A. Baker, D.D. Doyle, P. Geltenbort, K. Green, M.G.D. van der Grinten, P.G. Harris, P. Iaydjiev, S.N. Ivanov, D.J.R. May, J.M. Pendlebury, J.D. Richardson, D. Shiers, K.F. Smith, *Phys. Rev. Lett.* **97**, 131801 (2006)
143. R. Peccei, H. Quinn, *Phys. Rev. Lett.* **38**, 1440 (1977)
144. R. Peccei, H. Quinn, *Phys. Rev. D* **16**, 1791 (1977)
145. P. Sikivie, *Phys. Today* **49**, 22 (1996)
146. L.F. Abbott, P. Sikivie, *Phys. Lett. B* **120**, 133 (1983)
147. J. Preskill, M.B. Wise, F. Wilczek, *Phys. Lett. B* **120**, 127 (1983)
148. M. Dine, W. Fischler, *Phys. Lett. B* **120**, 137 (1983)
149. R.L. Davis, *Phys. Rev. D* **32**, 3172 (1985)
150. S. Chang, C. Hagmann, P. Sikivie, *Phys. Rev. D* **59**, 023505 (1998)
151. M. Nagasawa, M. Kawasaki, *Phys. Rev. D* **50**, 4821 (1994)
152. L.D. Duffy, K. van Bibber, *New J. Phys.* **11**, 105008 (2009)
153. G.G. Raffelt, *Annu. Rev. Nucl. Part. Sci.* **49**, 163 (1999)
154. P.W. Graham, A. Scherlis, *Phys. Rev. D* **98**(3), 035017 (2018)
155. F. Wilczek, *Phys. Rev. Lett.* **49**, 1549 (1982)
156. G. Gelmini, S. Nussinov, T. Yanagida, *Nucl. Phys. B* **219**, 31 (1983)
157. A. Ansel'm, *Pis'ma Zh. Eksp. Teor. Fiz.* **36**, 46 (1982)
158. J. Scherk, *Phys. Lett. B* **88**, 265 (1979)
159. D.E. Neville, *Phys. Rev. D* **21**, 2075 (1980)
160. D.E. Neville, *Phys. Rev. D* **25**, 573 (1982)
161. S.M. Carroll, G.B. Field, *Phys. Rev. D* **50**, 3867 (1994)
162. P. Svrček, E. Witten, *J. High Energy Phys.* **06**, 051 (2006)
163. P.W. Graham, D.E. Kaplan, S. Rajendran, *Phys. Rev. Lett.* **115**, 221801 (2015)
164. K. Harigaya et al., *Phys. Rev. Lett.* **124**, 111602 (2020)
165. R.T. Co, L.J. Hall, K. Harigaya, *J. High Energy Phys.* **2021**, 172 (2021)
166. S. Ge, K. Lawson, A. Zhitnitsky, *Phys. Rev. D* **99**, 116017 (2019)
167. D. Budker, V.V. Flambaum, X. Liang, A. Zhitnitsky, *Phys. Rev. D* **101**, 043012 (2020)
168. V.V. Flambaum, A.R. Zhitnitsky, *Phys. Rev. D* **99**, 023517 (2019)
169. M. Cvetič, P. Langacker, *Phys. Rev. D* **54**, 3570 (1996)
170. B. Holdom, *Phys. Lett. B* **166**, 196 (1986)
171. P. Langacker, *Rev. Mod. Phys.* **81**, 1199 (2009)
172. N. Arkani-Hamed, D.P. Finkbeiner, T.R. Slatyer, N. Weiner, *Phys. Rev. D* **79**, 015014 (2009)
173. P. Arias, D. Cadamuro, M. Goodsell, J. Jaeckel, J. Redondo, A. Ringwald, *J. Cosm. Astropart. Phys.* **2012**, 013 (2012)
174. A.E. Nelson, J. Scholtz, *Phys. Rev. D* **84**, 103501 (2011)
175. M.S. Safronova, D. Budker, D. DeMille, D.F. Jackson Kimball, A. Derevianko, C.W. Clark, *Rev. Mod. Phys.* **90**, 025008 (2018)
176. J.E. Moody, F. Wilczek, *Phys. Rev. D* **30**, 130 (1984)
177. B.A. Dobrescu, I. Mocioiu, *J. High Energy Phys.* **11**, 005 (2006)
178. P. Fadeev, Y.V. Stadnik, F. Ficek, M.G. Kozlov, V.V. Flambaum, D. Budker, *Phys. Rev. A* **99**, 022113 (2019)
179. H. Primakoff, *Phys. Rev.* **81**, 899 (1951)
180. G. Raffelt, D. Seckel, *Phys. Rev. Lett.* **60**, 1793 (1988)
181. R. Battesti, J. Beard, S. Böser, N. Bruyant, D. Budker, S.A. Crooker, E.J. Daw, V.V. Flambaum, T. Inada, I.G. Irastorza et al., *Phys. Rep.* **765**, 1 (2018)
182. D. Budker, P.W. Graham, M. Ledbetter, S. Rajendran, A.O. Sushkov, *Phys. Rev. X* **4**, 021030 (2014)

Open Access This chapter is licensed under the terms of the Creative Commons Attribution 4.0 International License (<http://creativecommons.org/licenses/by/4.0/>), which permits use, sharing, adaptation, distribution and reproduction in any medium or format, as long as you give appropriate credit to the original author(s) and the source, provide a link to the Creative Commons license and indicate if changes were made.

The images or other third party material in this chapter are included in the chapter's Creative Commons license, unless indicated otherwise in a credit line to the material. If material is not included in the chapter's Creative Commons license and your intended use is not permitted by statutory regulation or exceeds the permitted use, you will need to obtain permission directly from the copyright holder.

